Suggesting a di-omega dibaryon search in heavy ion collision experiments

Z. Y. Zhang and Y. W. Yu
Institute of High Energy Physics, 100039 Beijing, People's Republic of China

C. R. Ching and T. H. Ho
Institute of Theoretical Physics, 100080 Beijing, People's Republic of China

Z. D. Lu
China Institute of Atomic Energy, 102143 Beijing, People's Republic of China

The structure of a new dibaryon $(\Omega\Omega)_{0^+}$ is studied theoretically in the framework of the chiral SU(3) quark model by solving a resonating group method equation. The binding energy of this dibaryon is predicted to be around 100 MeV, the mean-square root of the distance between two Ω's is 0.84 fm, and the preliminary estimated mean lifetime is about two times that of the free Ω's. All these interesting properties, as well as the two negative charge units it carries, could make it easily identifiable experimentally in the heavy ion collision process. The production probability of this new dibaryon in a 158 GeV Pb+Pb collision is estimated using the thermal model. The rate is of the order of 10^{-6} to 10^{-5} per event. It is expected that, with the increase of the temperature, the production rate will also be increased.

I. INTRODUCTION

As is well known, in the ordinary strong interaction world there are only baryons consisting of three valence quarks and mesons of a quark-antiquark pair. However, for more than 20 years people have discussed and explored the possible existence of some exotic multiquark states and gluonic states, not only because it provides a good place to examine the quantum chromodynamics (QCD) theory and to display the quark-gluon behavior in short distance, but also the very existence of such systems would open a new area for studying many new physical phenomena we have not known before. But so far both the theoretical and the experimental efforts in searching for such systems have not been very successful. The theoretical investigations have concentrated mainly on H dihyperon [1–5] and d' particle [6,7], and there is also no convincing experimental evidence for the existence of these particles. This indicates, in seeking for multiquark system, or so-called dibaryon, that one probably should go beyond these few candidates to the multistrangeness systems.

Recently we have developed a chiral SU(3) quark model [8,9], in which the coupling between the chiral fields and quarks is considered to describe the medium range nonperturbative QCD effect. Since this model reproduced the energies of the baryon ground states, the nucleon-nucleon (N-N) scattering phase shifts and the hyperon-nucleon (Y-N) cross sections correctly, making an extrapolation in the same framework without introducing any new parameters to predict the dibaryons' structure is feasible and reliable to some extent. Using this model [10], an analysis of the six-quark states in $(0s)^6$ space has been made. We found that some six-quark states with high strange number have more attraction from the chiral quark coupling. Of particular interest is the $(\Omega\Omega)_{0^+}$: It is a deeply bound state (binding energy is around 100 MeV); the mean lifetime of this dibaryon is as long as about twice that of the free Ω lifetime, because it can

only exist through weak decay. This dibaryon has charge -2 and enough long mean lifetime, and therefore could be easily identified in the experiments.[1]

In this paper, we suggest to search for this exotic system in ultrarelativistic heavy ion collisions. In what follows we first give a brief introduction to our chiral SU(3) quark model. Then in Sec. III the main properties of dibaryon $(\Omega\Omega)_{0^+}$ are summarized with emphasis on the physics that leads to such interesting properties. In Sec. IV both the production probabilities of Ω^- and $(\Omega\Omega)_{0^+}$ are estimated using the thermal model. And finally in Sec. V some conclusions are presented.

II. A BRIEF INTRODUCTION OF THE CHIRAL SU(3) QUARK MODEL

In the usual quark potential model, the quark-quark interaction has only two parts: one-gluon-exchange (OGE) and confinement potential. This simple model is quite successful in explaining the heavy quarkonia. However, if applied to the light quark system, then one finds that the medium range nonperturbative effect has to be added, and the constituent quark mass must be put in phenomenologically. An alternative approach is to employ the SU(2) σ model [12,13]. In order to study the systems with strangeness, we have generalized the idea of the SU(2) σ model to the flavor SU(3) case, in which a unified coupling between quarks and all scalar and pseudoscalar chiral fields is introduced and the constituent quark mass can be obtained in principle as the

———

[1] Wang *et al.* also studied the $(\Omega\Omega)_{0^+}$ system by using a quark delocalization model [11]. They got the energy of $(\Omega\Omega)_{0^+}$ to be around the two Ω's threshold. But some serious problems in their calculation, as we have pointed out in Ref. [16], make their results unreliable.

consequence of spontaneous chiral symmetry breaking of the QCD vacuum [8]. With this generalization, the interacting Hamiltonian between quarks and chiral fields is now written as

$$H_I^{ch} = g_{ch} F(q^2) \bar{\psi} \left(\sum_{a=0}^{8} \sigma_a \lambda_a + i \sum_{a=0}^{8} \pi_a \lambda_a \gamma_5 \right) \psi, \quad (1)$$

where λ_0 is a unitary matrix, $\lambda_1 \cdots \lambda_8$ the Gell-Mann matrix of flavor SU(3) group, $\sigma_0 \cdots \sigma_8$ the scalar nonet fields, and $\pi_0 \cdots \pi_8$ the pseudoscalar nonet fields. $F(q^2)$ is a form factor,

$$F(q^2) = \left(\frac{\Lambda^2}{\Lambda^2 + q^2} \right)^{1/2}. \quad (2)$$

It is easy to show that H_I^{ch} is invariant under the SU(3) infinitesimal chiral transformation, and from H_I^{ch}, the chiral-field-induced quark-quark potential V_{ij}^{ch} between two quarks is derived, which describes the medium range nonperturbative effect.

The total Hamiltonian of the chiral SU(3) quark model is now obtained by adding to this Hamiltonian the OGE interaction as well as the confinement potential as follows:

$$H = \sum_i T_i - T_G + \sum_{i<j} V_{ij}, \quad (3)$$

where

$$V_{ij} = V_{ij}^{conf} + V_{ij}^{OGE} + V_{ij}^{ch} \quad (4)$$

and

$$V_{ij}^{ch} = \sum_{a=0}^{8} (V_{ij}^{S_a} + V_{ij}^{PS_a}), \quad (5)$$

where $\Sigma_i T_i - T_G$ is the kinetic energy of the system, T_G corresponds to the part of the center-of-mass motion, and V_{ij} is the interaction between two quarks. V_{ij}^{conf} is the confinement potential of quadratic form:

$$V_{ij}^{conf} = -a_{ij}^c (\lambda_i^c \lambda_j^c) r_{ij}^2,$$

and V_{ij}^{OGE} is the OGE interaction,

$$V_{ij}^{OGE} = \frac{1}{4} g_i g_j (\lambda_i^c \lambda_j^c) \left[\frac{1}{r_{ij}} - \frac{\pi}{2} \delta(\vec{r}_{ij}) \left(\frac{1}{m_i^2} + \frac{1}{m_j^2} \right. \right.$$
$$\left. \left. + \frac{4}{3} \frac{1}{m_i m_j} (\vec{\sigma}_i \cdot \vec{\sigma}_j) \right) \right].$$

V_{ij}^S and V_{ij}^{PS} stand for the scalar meson exchange and pseudoscalar meson exchange potentials, respectively [8],

$$V_{ij}^{S_a} = -\frac{g_{ch}^2}{4\pi} \frac{\Lambda^2 m_a}{\Lambda^2 - m_a^2} \left[Y(m_a r_{ij}) - \frac{\Lambda}{m_a} Y(\Lambda r_{ij}) \right] (\lambda_i^a \lambda_j^a), \quad (6)$$

TABLE I. Model parameters.

m_u (MeV)	313
m_s (MeV)	470
b_u (fm)	0.505
g_u	0.916
g_s	0.911
a_{uu}^c (Mev/fm^2)	53.87
a_{us}^c (Mev/fm^2)	69.30
a_{ss}^c (Mev/fm^2)	103.0
m_π (fm^{-1})/Λ_π (fm^{-1})	0.7/4.2
m_K (fm^{-1})/Λ_K (fm^{-1})	2.51/4.2
m_η (fm^{-1})/Λ_η (fm^{-1})	2.7/5.0
$m_{\eta'}$ (fm^{-1})/$\Lambda_{\eta'}$ (fm^{-1})	4.85/5.0
m_{σ_0} (fm^{-1})/Λ_{σ_0} (fm^{-1})	3.17/4.2
$m_{\sigma'}$ (fm^{-1})/$\Lambda_{\sigma'}$ (fm^{-1})	4.85/5.0
m_κ (fm^{-1})/Λ_κ (fm^{-1})	4.85/5.0
m_ϵ (fm^{-1})/Λ_ϵ (fm^{-1})	4.85/5.0
$g_{NN\pi}^2/4\pi$	13.67

$$V_{ij}^{PS_a} = \frac{g_{ch}^2}{4\pi} \frac{m_a^2}{12 m_q^2} \frac{\Lambda^2 m_a}{\Lambda^2 - m_a^2} \left[Y(m_a r_{ij}) - \frac{\Lambda^3}{m_a^3} Y(\Lambda r_{ij}) \right] (\vec{\sigma}_i \cdot \vec{\sigma}_j)$$
$$\times (\lambda_i^a \lambda_j^a), \quad (7)$$

m_a denotes the mass and Λ the cut mass of the chiral field, g_{ch} is the coupling constant between quark and chiral fields, and $Y(x)$ is the Yukawa function.

The above model was first tested by applying this model to studying the baryons and hyperons, or in other words, all ground states built out of three quarks including three different flavors. In order to do this, one needs some parameters as input. They are the constituent quark masses m_u (the m_d is assumed, as usual, to be equal to m_u), and m_s; the size parameter of nucleon b_u; the chiral field coupling constant g_{ch} is fixed using the following relation:

$$\frac{g_{ch}^2}{4\pi} = \frac{g_{NN\pi}^2}{4\pi} \frac{9}{25} \frac{m_u^2}{M_N^2}, \quad (8)$$

and $g_{NN\pi}^2/4\pi$ is taken to be the experimental value ≈ 14. Moreover, the masses of chiral mesons also should be introduced. We have taken the masses of chiral mesons to be the real mesons' mass except m_{σ_0}, which is chosen to be 625 MeV according to the relation $m_{\sigma_0}^2 = (2m_q)^2 + m_\pi^2$ [8]. To fix all the parameters, the masses of N, Δ, Λ, and Σ were used. As for the coupling constant of OGE, g_i, and the strength of the confinement potential, a_{ij}^c, they are strongly constrained by the baryons' masses and their stability conditions. The values of the parameters are listed in Table I. Once the parameters are determined, all the octet and decuplet baryons' masses can be reproduced in our model [5,10].

Now equipped with this model with all the parameters thus determined, we go further to study the two baryon systems on quark level dynamically by solving the resonating

group method (RGM) equation [14,15] of the Hamiltonian (3). In the RGM calculation, the trial wave function is taken to be

$$\Psi_{ST} = \sum_i c_i \Psi_{ST}^{(i)}(\vec{s}_i), \tag{9}$$

with

$$\Psi_{ST}^{(i)}(\vec{s}_i) = \mathcal{A}(\phi_A(\vec{\xi}_1, \vec{\xi}_2)_{S_A T_A} \phi_B(\vec{\xi}_4, \vec{\xi}_5)_{S_B T_B} \chi(\vec{R}_{AB} - \vec{s}_i)$$
$$\times \mathcal{R}_{CM}(\vec{R}_{CM}))_{ST}, \tag{10}$$

where A and B describe two clusters, and ϕ, χ, and $\mathcal{R}$ represent the internal, relative, and center-of-mass motion wave functions, respectively. $\vec{s}_i$ is the generator coordinate [15], and $\mathcal{A}$ is the antisymmetrization operator,

$$\mathcal{A} = 1 - \sum_{i \in A, j \in B} P_{ij}, \tag{11}$$

where P_{ij} is the permutation operator of the ith and jth quarks.

The results we obtained are quite encouraging. All the calculated N-N scattering phase shifts, the Y-N scattering, and reaction cross sections are in agreement with the experimental data [8]. Therefore, a unified description of the baryon structure and the baryon-baryon interaction is achieved in the framework of our model.

Another interesting attempt in investigating the six-quark systems is to study the structure of the six-quark systems as a whole. Then we have found that among all possible candidates, of particular interest is the two Ω dibaryon $(\Omega\Omega)_{0^+}$, which has led to this paper.

III. MAIN PROPERTIES OF THE $(\Omega\Omega)_{0^+}$ DIBARYON

A. Binding energy and wave function of $(\Omega\Omega)_{0^+}$

We have calculated the eigenenergy of the two Ω system by taking the same set of parameters that were used in our N-N and Y-N scattering calculations [8,10]. The results showed that, unlike the H dibaryon [5], d' [6], and the $\Delta\Delta$ dibaryon [16], $(\Omega\Omega)_{0^+}$ is a deeply bound state with a small root of mean-squared radius,

$$B_{(\Omega\Omega)_{0^+}} = -(E_{(\Omega\Omega)_{0^+}} - 2M_\Omega) = 116 \text{ MeV},$$

$$\text{rms} = \sqrt{\frac{1}{6} \sum_{i=1}^{6} \langle(\vec{r}_i - \vec{R}_{CM})^2\rangle} = 0.627 \text{ fm}, \tag{12}$$

where $B_{(\Omega\Omega)_{0^+}}$ denotes the binding energy and rms the root of mean-squared radius of the quark. Moreover, the relative motion wave function of two Ω's, $\chi(R_{\Omega\Omega})$, is also separated and drawn in Fig. 1. And the root of mean-squared distance between $\Omega - \Omega$, RMS $= \sqrt{\langle R_{\Omega\Omega}^2 \rangle} = 0.84$ fm, is obtained. These results have shown that $(\Omega\Omega)_{0^+}$ is a very interesting six-quark state, not only because of its huge binding energy, but also because of the quite short distance between $\Omega - \Omega$.
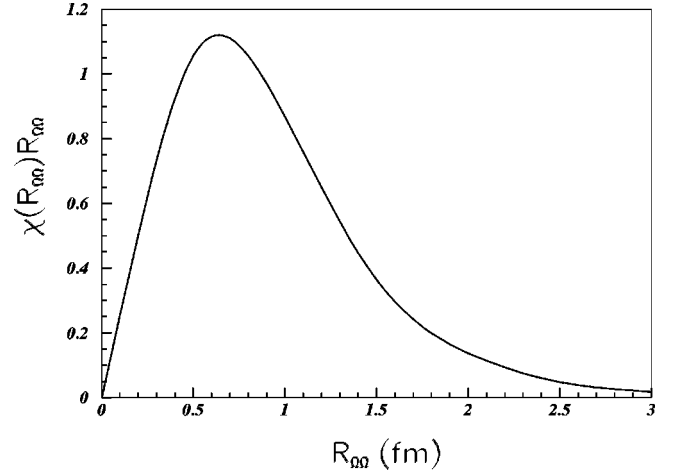
FIG. 1. Relative motion wave function of Ω-Ω.

This property, combined with the long lifetime, which we will see in Sec. III B, makes it the most favorable candidate for looking for the dibaryon.

To understand the very physics underlying the curious features, and to examine to what extent the results are dependent on the model with all its parameters we used, we have carried out an analysis of the interactions between quarks and the symmetry property of the system, and hence the interactions between two Ω's.

First let us discuss the symmetry property of this system, and its symmetry behavior in short distance.

As is well known, the composition of the baryon and the color magnetic interaction in the OGE potential govern the short-range region, and the RGM calculation with the OGE interaction can describe the short range behavior of the two baryons successfully. In the $(\Omega\Omega)_{0^+}$ case, although the OGE interaction is repulsive, the symmetry structure is very special. According to the transformation relations between the physical states of two baryons and the symmetry bases (group chain classification bases) of the six-quark system [17], one sees that among all 280 physical bases only six of them, namely $(\Delta\Delta)_{ST=30}$, $(\Delta\Delta)_{ST=03}$, $(\Delta\Sigma^*)_{ST=3(1/2)}$, $(\Delta\Sigma^*)_{ST=0(5/2)}$, $(\Xi^*\Omega)_{ST=0(1/2)}$, and $(\Omega\Omega)_{ST=00}$, have the largest component of $[6]_r$ symmetry in the orbital space of the symmetry bases, and $(\Omega\Omega)_{0^+}$ is one of them. According to our calculation in the frame of the chiral SU(3) quark model [10,16,18], all of these six states are bound with binding energies ranging from about several tens to hundreds of MeV. And what is remarkable is that among all others, $(\Omega\Omega)_{0^+}$ is the only state that is stable under the strong interaction.

On the other hand, as discussed in Ref. [19], the eigenvalue of the normalization kernel in the spin-flavor-color space $\langle \mathcal{A}^{\sigma f c} \rangle = \langle 1 - \Sigma_{i \in A, j \in B} P_{ij}^{\sigma f c} \rangle$ can serve as a direct measure on how the Pauli principle works in the relevant state. Or in other words, $\langle \mathcal{A}^{\sigma f c} \rangle$ is an important quantity describing the symmetry property of the state in the spin-flavor-color space. When $\langle \mathcal{A}^{\sigma f c} \rangle = 0$, it is a forbidden state for forming $[6]_r$ symmetry in the orbital space as a consequence of the Pauli exclusion principle. $\langle \mathcal{A}^{\sigma f c} \rangle = 1$ means the quark exchange effect between two baryons is unimpor-

tant; the two baryons can be regarded as two clusters without any quark exchange. When $\langle \mathcal{A}^{\sigma f c} \rangle$ is larger than 1, the quark exchange effect becomes cardinal, and tends to drag two clusters closer. Our calculation showed that for $(\Omega\Omega)_{0^+}, \langle \mathcal{A}^{\sigma f c} \rangle = 2$, so that $(\Omega\Omega)_{0^+}$ has relatively high antisymmetry in the spin-flavor-color space and symmetry in the orbital space, therefore it is favored by forming the $[6]_r$ symmetry basis.

With regard to how the symmetry property affects the binding energy, we have made an analysis by comparing $(\Omega\Omega)_{0^+}$ with deuteron. One first notes that, in contrast to the former, $\langle \mathcal{A}^{\sigma f c} \rangle$ is 10/9 for deuteron, i.e., it is slightly larger than 1, and almost half of that of the former. Furthermore, Fig. 2(a) shows the diagonal matrix elements of the Hamiltonian (3)–(7) in the generator coordinate method (GCM) calculation [15], which can describe qualitatively the interaction between two clusters, where s denotes the generator coordinate and $V_{\text{tot}}(s)$ is the effective potential of the two clusters. The solid curve represents the case of $(\Omega\Omega)_{0^+}$, and the dashed one is for the case of deuteron (only the central part). One sees that the potentials of these two states are quite different: $(\Omega\Omega)_{0^+}$ has a very deep potential with short range, while for deuteron the potential is shallow with relatively long range. To understand the main reason resulting in their difference, we further examined separately the potentials arising from the kinetic energy part $V_{\text{kin}}(s)$. [See Fig. 2(b). All symbols are the same as in Fig. 2(a).] For comparison, the corresponding potentials without quark exchange of the two Ω system are also shown in Fig. 2(b) as a dotted curve. From Fig. 2(b), one sees that, in contrast to the deuteron case, the $(\Omega\Omega)_{0^+}$ state has very strong attraction arising solely from the kinetic energy. Since the kinetic energy itself is spin-flavor-color independent, the big difference between $V_{\text{kin}}^{\text{deuteron}}(s)$ and $V_{\text{kin}}^{\Omega\Omega}(s)$ demonstrates clearly that the quantum-mechanical effect arising alone from the symmetry property has played a decisive role in binding the two clusters.

We have also performed a simplified model calculation, in which only the kinetic energy $\Sigma_i t_i - T_G$ and the color confinement potential V_{ij}^{conf} between quarks are taken into account. The result showed that $(\Omega\Omega)_{0^+}$ is bound with a binding energy as large as $B_{(\Omega\Omega)_{0^+}} = 17$ MeV. Since the color confinement almost does not contribute to the interaction between two color singlet clusters [19], this binding purely results from the quark exchange effect of the kinetic energy part, i.e., from the symmetry property of $(\Omega\Omega)_{0^+}$. Contrary to $(\Omega\Omega)_{0^+}$, having the antisymmetrization factor $\langle \mathcal{A}^{\sigma f c} \rangle = 10/9$ slightly larger than 1, the attraction arising from the quark exchange in the kinetic energy part for deuteron is very small [see the dashed curve in Fig. 2(b)]. The above presented analyses demonstrate that the symmetry property of $(\Omega\Omega)_{0^+}$ is crucial in forming a bound six-quark state.

Now for the chiral field coupling effect, first we have made a chiral SU(2) quark model calculation to see the contribution from the σ_0 exchange quantitatively, with $V^{\text{conf}}, V^{\text{OGE}}, V^{\pi}$, and V^{σ_0} included as the potential. The binding energy of $(\Omega\Omega)_{0^+}$ in this case is larger than 50 MeV [see case (IV) in Table II], while for the deuteron case the
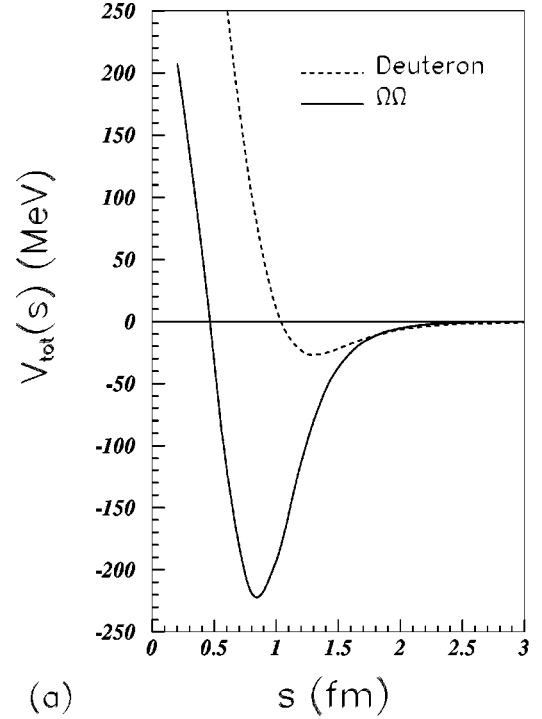
(a)
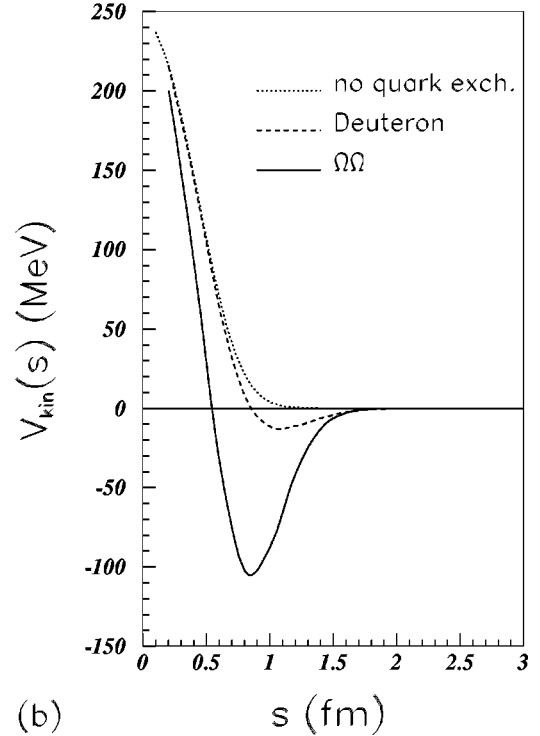
(b)

FIG. 2. (a) The GCM matrix elements of total Hamiltonian; (b) the GCM matrix elements of kinetic energy.

binding energy is only 2 MeV, as the experimental data have dictated. That means that even in the framework of SU(2), the theoretical calculation predicts that the binding energy of $(\Omega\Omega)_{0^+}$ is almost 20 times bigger than that of deuteron's.

Furthermore, we have examined the effects from the other chiral field coupling. For this purpose, several calculations with different chiral fields were carried out. The results are

TABLE II. Binding energies and RMS of $(\Omega\Omega)_{0^+}$ for different cases ($m_u = 313$ MeV, $m_s = 470$ MeV, $b_u = 0.505$ fm, $m_\sigma = 625$ MeV).

| | Chiral SU(3) quark model | | $\pi, k, \eta, \eta' + \sigma_0$ model | Chiral SU(2) quark model |
| | $m_\epsilon = m_\kappa = 958$ (MeV) | $m_\epsilon = m_\kappa = 1400$ (MeV) | | |
	(I)	(II)	(III)	(IV)
$B_{(\Omega\Omega)_{0^+}}$ (MeV)	116	99	74	54
RMS (fm)	0.84	0.85	0.92	0.98

listed in Table II. As mentioned before, for the chiral SU(2) case (only π and σ_0 are considered), $B_{(\Omega\Omega)_{0^+}} = 54$ MeV [see Table II, case (IV)]. Then we include the exchange of all pseudoscalar mesons plus σ_0. The result shows that when π, K, η, η', and σ_0 chiral fields are added, $B_{(\Omega\Omega)_{0^+}} = 74$ MeV [see Table II, case (III)]. Finally, with the inclusion of the exchange of all nonet pseudoscalar and scalar mesons in our calculation, i.e., the chiral SU(3) quark model, the binding becomes even stronger. The results are shown as cases (I) and (II) in Table II. Case (I) is the earliest one, in which the parameters are taken to be the same as we used in N-N and Y-N calculation [8]. One sees that besides σ_0, the effect from the other scalar mesons (σ', κ, and ϵ) also enhances the binding in the $(\Omega\Omega)_{0^+}$ system. The total binding energy reaches 116 MeV when these scalar mesons are included [see Table II, case (I)]. (For deuteron the inclusion of these mesons leads to a small change in the binding energy.)

Since the N-N and N-Y systems are insensitive to the masses of κ and ϵ mesons, and in order to reduce the number of adjustable parameters, $m_\epsilon = m_\kappa = m_{\eta'} = 958$ MeV (around 1000 MeV) is used in the calculation [8]. But now for the $\Omega\Omega$ case, a six-strange-quark system, both the values of m_ϵ and m_κ may be important and should be retested. Therefore, we have adopted another value for the masses as $m_\epsilon = m_\kappa = 1400$ MeV, and the calculated result is shown as case (II) in the second column of Table II. As we expected, when the mass of ϵ increases, the attraction from ϵ is reduced, and so is the binding energy. But the property of strong binding of the system remains. All these analyses and calculations point to the fact that both the specific symmetry property of the system $(\Omega\Omega)_{0^+}$, or in other words, the quark exchange effect in the short range, and the nonperturbative QCD effect described by chiral-quark coupling (especially the σ_0 exchange) in the medium range, are responsible for forming a deeply bound state of $(\Omega\Omega)_{0^+}$ with the binding energy ranging between 50 MeV and 115 MeV.

The calculations were also performed with different size parameter b_u and strange quark mass m_s. The results are shown in Fig. 3, in which the solid curve represents the case of $m_s = 470$ MeV, the dashed curve $m_s = 500$ MeV, and dotted one $m_s = 550$ MeV. One sees that with the relevant parameters varying in a maximum allowable region, the binding energy $B_{(\Omega\Omega)_{0^+}}$ are between 60 and 140 MeV. In general, when b_u is taken to be 0.50–0.55 fm, and m_s to be 470–520 MeV, the data of the N-N scattering and the Y-N

cross section can be roughly fitted [8,20,21], and given the parameters in this range, the variations of $B_{(\Omega\Omega)_{0^+}}$ are limited, and the binding energy is 100 ± 15 MeV. This means that our result is not very sensitive to the used parameters.

Here we would like to note that in our calculation, the confinement potential has no influence on the results, because in a single-channel RGM calculation, the color confinement potential almost does not give any interactions between two color-singlet $(0s)^3$ clusters. Therefore, we say the quark exchange effect and the chiral-quark coupling play the dominant role in forming the $(\Omega\Omega)_{0^+}$ as a deeply bound six-quark state.

B. Mean lifetime of $(\Omega\Omega)_{0^+}$

When we deal with the decay of $(\Omega\Omega)_{0^+}$, two facts play a dominant role in the process. The first one is the large binding energy of the system, and the second is the quantum number strangeness $\mathcal{S}(\mathcal{S} = -6)$. The latter, in particular, results in $(\Omega\Omega)_{0^+}$ only undergoing weak decay. Furthermore, the selection rule $\Delta\mathcal{S} = 1$ in the weak process means that $(\Omega\Omega)_{0^+}$ can split into three particles: an Ω plus another hyperon plus pions or leptons that are determined by the decay modes of a free Ω. In addition to these conventional decay modes, there also exists a very interesting two particle decay mode:

$$(\Omega\Omega)_{0^+} \rightarrow \Omega^- + \Xi^-,$$
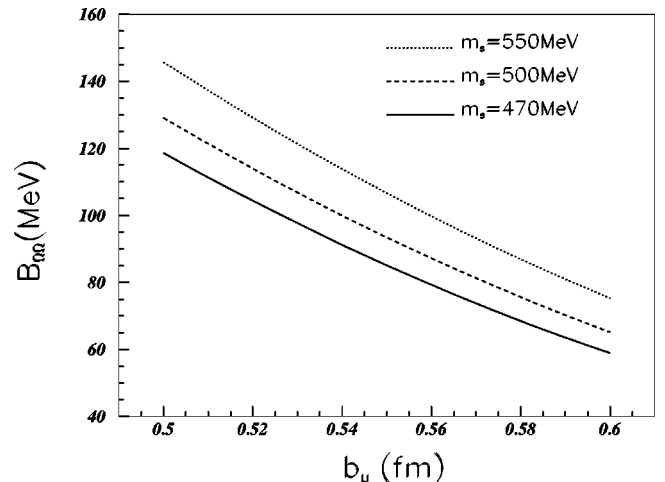
FIG. 3. Binding energy of $(\Omega\Omega)_{0^+}$ vs b_u and m_s.
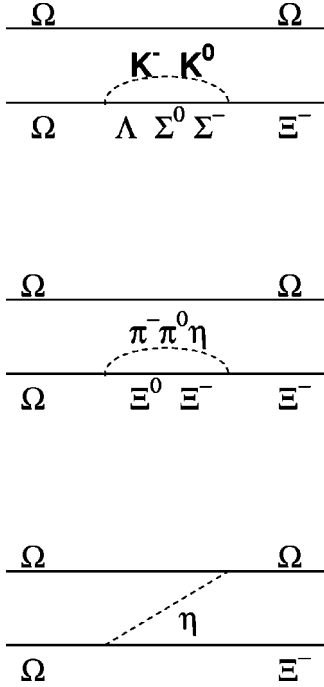
FIG. 4. Two-body decay Feynman diagram.

and the corresponding Feynman diagrams are depicted in Fig. 4.

Since it was well established that, for free Ω, the most important decay modes are [22] ΛK^-, $\Xi^0 \pi^-$, and $\Xi^- \pi^0$, now if the binding energy of about 100 MeV is taken into account, the decay channel $\Omega + \Lambda + K^-$ is forbidden strictly by energy conservation. And therefore only two decay channels remain, namely,

$$(\Omega\Omega)_{0^+} \rightarrow \Omega^- + \Xi^0 + \pi^-$$

and

$$(\Omega\Omega)_{0^+} \rightarrow \Omega^- + \Xi^- + \pi^0.$$

Then this partial width of the bound state of $(\Omega\Omega)_{0^+}$ can be estimated under the sudden approximation as we did for calculating the β spectrum of the tritium molecule decay [23,24]. In this calculation, the above-mentioned processes can be regarded as a transition between two ''molecules'': $(\Omega\Omega)_{0^+}$ and $(\Omega\Xi)$. The latter, as shown in Ref. [10], can also form a loosely bound state with a binding energy about several MeV. However, owing to the sudden interaction change occurring in the weak decay process, the newly formed complex system $(\Omega\Xi)$ does not necessarily stay in its ground state. Instead, all the excited states, including the continuous ones, in accordance with the selection rules contribute to the transition with the weight, which is determined by the overlapping of the wave functions of the two compound systems. As a result, the expression for the decay probability of the free Ω is modified.

The free Ω decay probability is known as [25]

$$\Gamma = \frac{q^3}{12\pi M_\Omega m_\pi^2}(m' + E)B^2, \tag{13}$$

where q is the momentum of the produced kaon or pion, M_Ω, m_π, and m' are, respectively, the rest mass of Ω, charged pion, and of the decay-produced hyperon, E is the total energy of this hyperon, and B is a constant, describing the p-wave amplitude, which is known from the experiments for each decay mode.

For the case when both the initial and final hyperons are sitting in the complex systems, the expression for the transition rate now reads as

$$\Gamma = \sum_n \langle f_n | i \rangle^2 \frac{q_{i,f_n}^3}{12\pi M_\Omega m_\pi^2}[m' + E(i,n)]B^2, \tag{14}$$

where all the quantities with the indices i and f_n are now referred to the same quantities as in Eq. (13) but with the values corresponding to the transition between initial state i and the final state n, respectively.

To estimate the transition rate of $(\Omega\Omega)_{0^+}$, the closure approximation can be used [24]. This means that we replace in Eq. (14) the pion momentum q_{i,f_n} and the corresponding hyperon energy $E(i,n)$ by the average values, respectively. Then, instead of Eq. (14) one gets

$$\Gamma = \sum_n \langle f_n | i \rangle^2 \frac{\bar{q}^3}{12\pi M_\Omega m_\pi^2}(m' + \bar{E})B^2$$

$$= \frac{\bar{q}^3}{12\pi M_\Omega m_\pi^2}(m' + \bar{E})B^2, \tag{15}$$

where $\bar{E} = \sqrt{(m'^2 + \bar{q}^2)}$ and $\bar{q} = \Sigma_n \langle f_n | i \rangle^2 q_{i,f_n}$.

Since among all the possible final states of the system $(\Xi\Omega)$ the ground-to-ground-state transition gives rise to the largest pion momentum q, and hence the largest decay rate, and since we are interested in the lower bound of the lifetime of $(\Omega\Omega)_{0^+}$, we may therefore use the q value of the ground-to-ground-state transition for estimating the decay rate safely. Thus, after taking into account the binding energy of ≈ 100 MeV for the $(\Omega\Omega)_{0^+}$ [the binding energy for the $(\Xi\Omega)$ system here is neglected], we have the following q values for two decay modes, respectively:

$$q = 207 \text{ MeV}, \quad B = 1.86 \times 10^{-7}$$

$$\text{for } (\Omega\Omega)_{0^+} \rightarrow (\Xi^0\Omega^-) + \pi^-, \tag{16}$$

and

$$q = 203 \text{ MeV}, \quad B = 1.14 \times 10^{-7}$$

$$\text{for } (\Omega\Omega)_{0^+} \rightarrow (\Xi^-\Omega^-) + \pi^0, \tag{17}$$

where the B values are taken to be that of free Ω decay [25]. With these values, and using Eq. (15), the three-body decay width of $(\Omega\Omega)_{0^+}$ can be easily obtained, which is four times smaller than that of free Ω's.

In comparing with the above discussed three-body decay, it is much more complicated to calculate the two-body decay of $(\Omega\Omega)_{0^+}$. Phenomenologically one can introduce an effective coupling constant A, describing the p-wave parity-violating part in the nonleptonic decay amplitude of hyperon. Then the decay width of $(\Omega\Omega)_{0^+}\rightarrow\Omega+\Xi$ can be obtained as

$$\Gamma=\frac{A^2q'^3(m_1+E_1')(m_2+E_2')}{3m_\pi^2M_i^2}R^2,$$

where m_1 and m_2 stand for the masses of final Ω and Ξ, respectively, and E_1',E_2' their energies; R is the overlapping integral of the wave function of $(\Omega\Omega)_{0^+}$ and the plane wave of the final particles. Given the binding energy of 100 MeV, we have $q'=624$ MeV/c; then $R=0.11$. Therefore, the gain from the phase space is suppressed totally by the R^2. Assuming that $A\simeq B$, then the width of two-body decay is almost the same as that of three-body decay given by Eq. (15). Taking all of them together, the preliminarily estimated lifetime for $(\Omega\Omega)_{0^+}$ is about two times longer than that of a free Ω. As a matter of fact, the free Ω lifetime is 0.822×10^{-10} s [22].

However, it should be stressed that the lifetime is binding-energy-dependent. In particular, the two-body decay rate depends on the overlapping integral of the wave function sensitively. Moreover, measuring this interesting decay mode becomes the most straightforward way to determine the binding energy of the $(\Omega\Omega)$ system accurately, and at the same time it will provide valuable information concerning some pieces of the nonleptonic weak amplitude of baryon, which is missing in the usual Ω decay.

IV. PRODUCTION PROBABILITY OF Ω^- AND $(\Omega^-\Omega^-)$

In the past decade, many features of the experimental data accumulated in ultrarelativistic collision between heavy nuclei at AGS and SPS seem to indicate that a large degree of thermal and chemical equilibrium is reached among the produced hadrons [26–28]. Therefore, as a preliminary and crude estimate, the thermal model is used to describe the heavy ion collision, and based on it, the $(\Omega\Omega)_{0^+}$ production rate is estimated.

In this section, we use the thermal model [27–29] to calculate the production probability of Ω^- and estimate the production probability of $(\Omega^-\Omega^-)$ in 158A GeV Pb+Pb collision.

According to the thermal model of heavy ion collision, a fireball with extreme high temperature and extreme high density is formed. After reaching the highest density and temperature, the fireball undergoes the expansion until freeze-out. The production of a large amount of particles and the violent collisions between them in the fireball finally lead to the thermal and chemical equilibrium soon after it reaches the highest density and highest temperature. The thermal

TABLE III. Multiplicity of $\Lambda+\bar\Lambda$, $\Xi^-+\bar\Xi^+$, and $\Omega^-+\bar\Omega^+$. The calculation results are obtained at $T\approx110$ MeV and $\rho_B/\rho_0\approx0.1$. The experimental data are adopted from Ref. [30].

N_{part}		$\Lambda+\bar\Lambda$	$\Xi^-+\bar\Xi^+$	$\Omega^-+\bar\Omega^+$
350	cal.	18.1	1.47	0.155
	exp.	19.0	1.90	0.49
285	cal.	14.6	1.23	0.130
	exp.	15.0	1.6	0.38
220	cal.	11.0	0.816	0.081
	exp.	11.0	1.1	0.22
125	cal.	6.68	0.488	0.052
	exp.	7.0	0.59	0.13

equilibrium and chemical equilibrium are supposed to be maintained until freeze-out.

The statistical properties of the fireball are determined by the thermodynamic potential. The thermodynamic potential per unit volume for i species reads

$$\Omega_i=-\xi_i\frac{g_iT}{(2\pi)^3}\int d^3q\,\ln(1+\xi_ie^{\beta(\mu_i-\epsilon)}),\qquad(18)$$

where T is the temperature of the fireball and $\beta=1/T$. $\epsilon=\sqrt{q^2+m_i^2}$ is the energy of the particle. μ_i stands for the chemical potential for both baryons and mesons with and without strangeness. It is noted that μ_i depends on the temperature T and the ratio of baryon density ρ_B/ρ_0 (where ρ_B is the pure baryon density and ρ_0 is the normal nuclear density) of the hadronic gas. ξ_i stands for the statistics kind of particles, $\xi_i=1$ is for fermions, and -1 for bosons. The integration is carried out in the momentum space q.

With the thermodynamic potential, all thermodynamic quantities can be derived. The density of a particle of a given species is the partial differentiation of the corresponding chemical potential. For i species, the density is $\rho_i=-\partial\Omega/\partial\mu_i|_T$.

Since the temperature of the fireball is very high, it is reasonable to treat the hadron gas as the ideal gas with the Boltzmann distribution. At $\beta m\gg1$, the density of i species is

$$\rho_i=g_i\left(\frac{m_i}{2\pi\beta}\right)^{3/2}e^{-\beta(m_i-\mu_i)},\qquad(19)$$

where m_i is the mass and g_i is the spin-isospin degeneracy. The multiplicity of each particle can thus be obtained by integrating the corresponding density in the coordinate space.

Since the above-mentioned thermal model can reproduce the experimental data of the particle ratio and the kaon and pion production in SPS heavy ion collisions [27–29], it is therefore very important to check whether this model can also well reproduce the data of hyperon. We have made the calculation for hyperon production in 158A GeV Pb+Pb collision and compared it with the experimental data. The model calculations as well as the experimental data are shown in Table III. The first column, N_{part}, is the number of
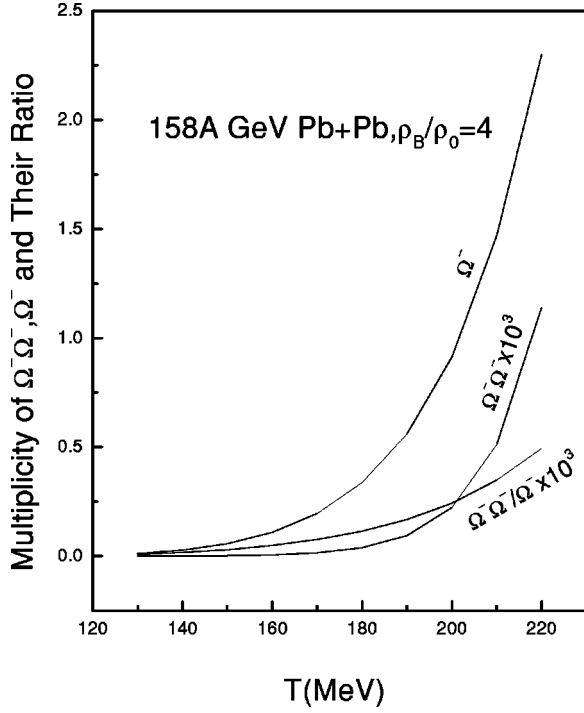
FIG. 5. Multiplicity of $\Omega^-\Omega^-$, Ω^-, and their ratio vs T (MeV).

FIG. 6. Multiplicity of $\Omega^-\Omega^-$, Ω^-, and their ratio vs ρ_B/ρ_0.

participants related to the impact parameter. Other columns are $\Lambda+\bar{\Lambda}$, $\Xi^-+\bar{\Xi}^+$, and $\Omega^-+\bar{\Omega}^+$, respectively. The experimental data are adopted from Ref. [30]. The agreement seems reasonable. The fitting to the experimental data is carried out at freeze-out. From the fits, we obtain the freeze-out temperature to be about 110 MeV and the freeze-out baryon density to be about $0.1\rho_0$, which are the same as that obtained in 200A GeV S+S and S+Ag collisions [29].

The multiplicity of Ω^- are shown in Figs. 5 and 6 as a function of T and ρ_B/ρ_0 in 158A GeV Pb+Pb collision. The multiplicity, as expected, increases as the temperature increases, while it decreases as baryon density increases. For convenience of illustration, we take $T=160$ MeV and $\rho_B/\rho_0=4$ to be the reference point in 158A GeV Pb+Pb collision. Figure 5 is for $\rho_B/\rho_0=4$; the multiplicity of Ω^- increases from 2.8×10^{-2} to 3.4×10^{-1} as the temperature increases from 140 MeV to 180 MeV. Figure 6 is for $T=160$ MeV; the multiplicity of Ω^- decreases from 2.5 $\times10^{-1}$ to 6.4×10^{-2} as the ρ_B/ρ_0 increases from 2 to 6.

Given the above-obtained results, we are now in a position to give a preliminary and rough estimate for the multiplicity of $\Omega^-\Omega^-$ from the multiplicity of Ω^- based on the same model. Since $\Omega^-\Omega^-$ is a six-strange-quark cluster and the binding energy for two Ω^-'s to form a $\Omega^-\Omega^-$ cluster is about 110 MeV, the mass of this cluster is about 3230 MeV, and hence the production rate is much lower than the other particles. It is reasonable to assume that the inclusion of this particle would cause little effect to the other particles in the original calculations. Therefore, the multiplicity of $\Omega^-\Omega^-$ can be estimated directly from that of Ω^-.

From formula (19), the ratio of $\Omega^-\Omega^-$ to Ω^- is
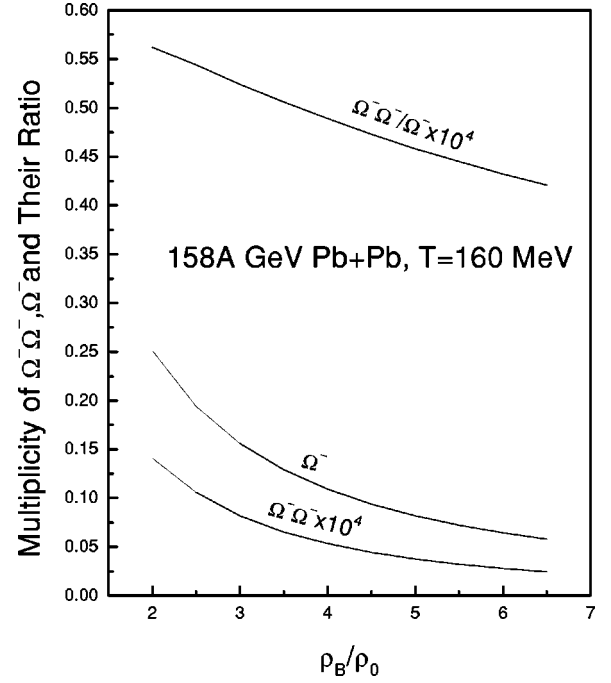
$$r=\frac{g_{\Omega^-\Omega^-}}{g_{\bar{\Omega}}}\left(\frac{m_{\Omega^-\Omega^-}}{m_{\bar{\Omega}}}\right)^{3/2}e^{-\beta[(m_{\Omega^-\Omega^-}-\mu_{\Omega^-\Omega^-})-(m_{\Omega^-}-\mu_{\Omega^-})]}.$$

(20)

The chemical potential of $\Omega^-\Omega^-$ is six times of the chemical potential of a strange quark. The chemical potential of a strange quark, μ_s, is quite small for high temperature and decreases very fast as temperature increases. For instance, at $\rho_B/\rho_0=4$, μ_s is lowered from 25.3 MeV to -1.59 MeV as temperature increases from 140 MeV to 180 MeV. At reference point, i.e., $T=160$ MeV and $\rho_B/\rho_0=4$, the chemical potential of the strange quark is 10.9 MeV. Compared to the huge mass, the effect of the chemical potential on $\Omega^-\Omega^-$ production can be neglected.

The ratio of $\Omega^-\Omega^-$ to Ω^- together with the multiplicity of $\Omega^-\Omega^-$ are also shown in Figs. 5 and 6. The ratio increases for higher temperatures and for lower baryon densities. As a result, the multiplicity of $\Omega^-\Omega^-$ will increase as temperature increases and decrease as baryon density increases. At $\rho_B/\rho_0=4$, the multiplicity of $\Omega^-\Omega^-$ increases from 4.7×10^{-7} to 1.5×10^{-5} as the temperature increases from 140 MeV to 180 MeV. At $T=160$ MeV, the multiplicity of $\Omega^-\Omega^-$ is from 1.4×10^{-5} to 2.8×10^{-6} for ρ_B/ρ_0 from 2 to 6. At reference point, the multiplicity of $\Omega^-\Omega^-$ is 5.3×10^{-6}.

The above results are deduced from that of 158A GeV Pb+Pb collision. They are very sensitive to the temperature and the baryon density. For higher temperature that can be achieved in the future RHIC and LHC, it can be expected that more $\Omega^-\Omega^-$ can be produced.

V. DISCUSSIONS AND CONCLUSIONS

In the preceding sections we have shown that $(\Omega\Omega)_{0^+}$ is a deeply bound dibaryon with a binding energy about 40

times larger than that of the deuteron's. The root of mean-squared radius of quark distribution of $(\Omega\Omega)_{0^+}$ is only about half that of the deuteron. Such remarkable features are predominantly originated from its special symmetry properties. This can be seen by recalling that the kinetic energy alone contributes 17 MeV to the binding energy. The symmetry property is further coupled with meson exchange potentials, and finally results in about 100 MeV binding energy for the $(\Omega\Omega)_{0^+}$ system. Judging by these features, $(\Omega\Omega)_{0^+}$ is a six-quark state rather than a normal two-baryon bound state. The deuteron is a bound state of another kind: its symmetric structure prevents the exchange of quarks between the two baryons, and the baryons preserve their individuality. Thus, deuteron is a loosely bound state. This symmetry property analysis is quite general, and is, in fact, irrelevant to any specific model, except for the quark model of baryon.

However, the concrete value of the binding energy depends on the input parameters, or in other words, it is model-dependent. It should be noted that when using the chiral SU(3) quark model, our approach is mostly phenomenological. By fitting with a large body of the experimental data concerning the baryon and hyperon structures and scattering cross sections, the set of parameters we have chosen is optimized and the range of variations is also known. It seems that, within a widely allowable range of variations of the parameters, our numerical results do not alter very much.

The most preferable value obtained for the binding energy is 100 MeV $\pm$ 15 MeV.

Besides the binding energy, another important and interesting property is the lifetime of $(\Omega\Omega)_{0^+}$. As we have discussed in the previous sections, because of the large strangeness quantum number of this system, only weak decay is allowed. If the binding energy is chosen to be 100 MeV, as a preliminary estimate, the lifetime could be about two times that of the free Ω's.

Our estimates for the production rate of $(\Omega\Omega)_{0^+}$ are also very crude and preliminary. If the experimental suggestion is under consideration, a more detailed calculation and simulation should be done.

As a conclusion, we believe $(\Omega\Omega)_{0^+}$ is the best candidate to look for the long-sought dibaryon. Last but not least, once such a system is observed experimentally, the binding energy deduced from the experiment may justify the model used for the calculation.

[1] R.J. Jaffe, Phys. Rev. Lett. **38**, 195 (1977).

[2] M. Oka, K. Shimizu, and K. Yazaki, Phys. Lett. **130B**, 365 (1983); Nucl. Phys. **A464**, 700 (1987); K. Shimizu and M. Koyama, *ibid.* **A646**, 211 (1999).

[3] U. Straub, Zong-ye Zhang, K. Bräuer, A. Faessler, and S.B. Khadkikar, Phys. Lett. B **200**, 241 (1988).

[4] K. Imai, Nucl. Phys. **A553**, 667 (1993).

[5] P.N. Shen, Z.Y. Zhang, Y.W. Yu, X.Q. Yuan, and S. Yang, J. Phys. G **25**, 1807 (1999).

[6] A.J. Buchmann *et al.*, Prog. Part. Nucl. Phys. **36**, 383 (1996); Phys. Rev. C **57**, 3340 (1998).

[7] H. Clement *et al.*, Prog. Part. Nucl. Phys. **36**, 369 (1996).

[8] Z.Y. Zhang, Y.W. Yu, P.N. Shen, and L.R. Dai, Nucl. Phys. **A625**, 59 (1997).

[9] P.N. Shen, Y.B. Dong, Y.W. Yu, Z.Y. Zhang, and T.S.H. Lee, Phys. Rev. C **55**, 2024 (1997).

[10] Y.W. Yu, Z.Y. Zhang, and X.Q. Yuan, Commun. Theor. Phys. **31**, 1 (1999); Z.Y. Zhang, Y.W. Yu, and X.Q. Yuan, Nucl. Phys. A (to be published).

[11] F. Wang, J.L. Ping, G.H. Wu, L.J. Teng, and T. Goldman, Phys. Rev. C **51**, 3411 (1995).

[12] M. Gell-Mann and M. Levy, Nuovo Cimento **XVI**, 705 (1960).

[13] F. Fernandez, A. Valcarce, U. Straub, and A. Faessler, J. Phys. G **19**, 2013 (1993).

[14] J.A. Wheeler, Phys. Rev. **52**, 1083 (1937); **52**, 1107 (1937).

[15] K. Wildermuth and Y.C. Tang, *A Unified Theory of the Nucleus* (Vieweg, Braunschweig, 1977).

[16] X.Q. Yuan, Z.Y. Zhang, Y.W. Yu, and P.N. Shen, Phys. Rev. C **60**, 045203 (1999).

[17] M. Harvey, Nucl. Phys. **A352**, 301 (1981); F. Wang, J.L. Ping, and T. Goldman, Phys. Rev. C **51**, 1648 (1995).

[18] Q.B. Li, P.N. Shen, Z.Y. Zhang, and Y.W. Yu (unpublished).

[19] K. Shimizu, Prog. Phys. **52**, 1 (1989).

[20] S. Yang, P.N. Shen, Z.Y. Zhang, and Y.W. Yu, Nucl. Phys. **A635**, 146 (1998).

[21] Z.Y. Zhang, A. Faessler, U. Straub, and L. Ya. Glozman, Nucl. Phys. **A578**, 573 (1994).

[22] Particle Data Group, C. Caso *et al.*, Euro. Phys. J. C **3**, 1 (1998).

[23] A.B. Migdal, *Qualitative Methods in Quantum Theory*, translated by A.J. Leggett (Benjamin, New York, 1977), p. 102.

[24] C.R. Ching and T.H. Ho, Phys. Rep. **112**, 1 (1981).

[25] J.F. Donoghue *et al.*, Phys. Rep. **131**, 321 (1986).

[26] J. Stachel, Nucl. Phys. **A610**, 509c (1996).

[27] P. Braun-Munzinger and J. Stachel, Nucl. Phys. **A638**, 3c (1998).

[28] P. Braun-Munzinger *et al.*, Phys. Lett. B **365**, 1 (1996).

[29] Z.D. Lu *et al.*, High Energy Phys. Nucl. Phys. **22**, 910 (1998).

[30] E. Anderson *et al.*, Phys. Lett. B **433**, 209 (1998).